J Mater Sci (2019) 54:10728–10736

Computation and theory

Atomistic simulations of carbon effect on kink-pair energetics of bcc iron screw dislocations

Yinan Wang[1], Xiaoyang Wang[1], Qiulin Li[1,2], Ben Xu[1,*], and Wei Liu[1,*]

[1] *Key Laboratory of Advanced Materials (MOE), School of Material Science and Engineering, Tsinghua University, Beijing 100084, People's Republic of China*

[2] *Joint Laboratory of Nuclear Materials and Service Safety, Graduate School at Shenzhen, Tsinghua University, Shenzhen 518055, People's Republic of China*

Received: 15 January 2019
Accepted: 22 March 2019
Published online: 29 April 2019

© Springer Science+Business Media, LLC, part of Springer Nature 2019

ABSTRACT

The mechanical properties of body-centered cubic metals at low temperatures are strongly influenced by the solute atoms, which could be relatively complex as either hardening or softening effects would be introduced depending on the solute concentration and temperature. One major impact is that solute atoms can affect both kink formation and motion during screw dislocation gliding, which plays an important role in plastic behavior of bcc metals. In this study, atomistic simulations are conducted on the carbon-affected kinking of a screw dislocation in iron using the nudged elastic band method. When kink nucleates alongside a carbon atom, the kink formation energy decreases as the carbon transits to a stronger binding site, and vice versa. When a single kink meets the carbon during propagation, the sideward motion of the kink is impeded. With regard to the different temperatures and solute concentrations, the softening and hardening effects induced by carbon solutes in iron can be explained by the complex atomistic process.

Introduction

In body-centered cubic (BCC) metals, plastic deformation is controlled by the sliding of screw dislocations [4, 30, 32]. The limiting factor of such process is the thermally activated kink formation and propagation, which further restrict the motion of a/2[111] screw dislocation [7, 10, 20, 22, 31]. Numerous theoretical studies with molecular dynamics (MD) have been conducted to investigate the gliding mechanisms of screw dislocations (e.g., in BCC Fe at finite temperatures [8, 10, 16]). Narayanan et al. [17] employed the nudged elastic band (NEB) method to simulate the mechanisms of the thermally activated screw dislocation gliding, as well as the atomistic material parameters, and a single-humped reaction pathway was discovered. The kink-limited Orowan strengthening mechanism was modified by Swinburne et al. [26] to illustrate the thermally activated, kink-dominated glide of 1/2[111] screw dislocations,

Address correspondence to E-mail: xuben@mail.tsinghua.edu.cn; liuw@tsinghua.edu.cn

https://doi.org/10.1007/s10853-019-03564-y

enabling its application to the plastic deformation of BCC metals. Becquart discussed the interaction of a C atom with bcc Fe screw dislocation at 100 K employing dynamical simulations and observed three types of behaviors: screw dislocation keeps moving on its gliding plane; the cross-slip of dislocation and carbon jumping to an adjacent octahedral site [3]. Though the influence of the C atom on the slip plane of the screw dislocation is revealed, it is worth discussing more on how the C atom affects the mobility of the screw dislocation.

The mechanical properties of BCC metals at low temperatures have strong dependence on the concentration of solute elements. Even with a low content of solute elements the mechanical properties may change significantly. In BCC iron, the effects of solute elements on the mechanical properties are quite complex, and the results can be either hardening or softening. It is usually determined by the various types of solutes, concentrations, and temperature conditions [6, 18]. Trinkle et al. proposed a solid solution softening model of plasticity by modifying the energy and stress scales of double-kink nucleation and kink migration enthalpy barriers when introducing the solute atoms to the dislocation system [27]. The solid solution softening and hardening can also be determined by a modified Orowan equation. In this theory, the transition from softening to hardening with increasing solute element concentration can be explained by the switch of the rate-limiting step, from the kink nucleation rate to kink propagation rate [14].

Thus far, direct atomistic results on carbon-induced kink formation energy and propagation barrier changes of BCC iron screw dislocation have been revealed little. In this study, we successfully determined the activation energy of the kink-pair mechanism of the 1/2[111] screw dislocation using the NEB method. We employed this method to study the effects of carbon solutes on the energetics of a kink-pair mechanism in BCC iron. Carbon-induced softening and hardening effects are then discussed based on the simulation results.

Method of simulation

To investigate the effect of carbon on the kink-pair mechanism of the screw dislocation, NEB calculations are performed using the widely used LAMMPS [19] code. NEB method defines the transition path as a string of replicas of the system which is connected one after another by springs and strung between the reactant and product states [12]. A minimum energy path (MEP) can then be obtained by relaxing replicas perpendicular to the path.

The X, Y, Z directions are aligned along the [112], $[1\bar{1}0]$, and $[11\bar{1}]$ directions in the bcc lattice, respectively. The periodic boundary condition is applied along $[11\bar{1}]$ and [112], whereas the boundary is set free on $[1\bar{1}0]$ direction. The size of the simulation box is 85 Å, 85 Å, and 642 Å in each dimension. The dislocation is introduced in the middle of the simulation system based on the anisotropic elastic displacement fields [13], which is then relaxed as the initial state of the NEB simulation. An isolated screw dislocation having the same properties is created in another bulk system as the final state of the NEB simulation, which is one step away from the initial state in the [112] direction. Regarding the middle image, Becquart's potential predicts a metastable configuration during the gliding of the screw dislocation, as displayed in image 24 of Fig. 1a. If the initial and final states are provided without the middle configuration, the potential will predict the similar gliding process as Fig. 6 in Gordon's work [11], which is not accurate according to Narayanan's work [17]. This part of simulation is displayed in Fig. 1. The kink formation barrier is 11 meV/b larger than the process with a middle structure, as displayed in Fig. 2d. The middle image consists of half the length of the dislocation line of the initial and final states, which is a kink pair created manually. Therefore, a manually constructed a double kink is introduced as the middle structure. The influences of the instability of the hard configuration core energy predicted by the potential on the kink formation and motion energies are eliminated as a consequence.

The binding sites of the carbon atoms around the screw dislocation core as well as the binding energies have been previously discussed [9]. Figure 1 displays the Fe screw dislocation core with carbon interstitials. In this simulation, eight binding sites for carbon are considered, as A1 and A2 possess the same energy in the initial and final states. For B1, B2, and B3, the carbon transits from a stronger to a weaker binding site, whereas for C1, C2, and C3, the carbon transits from a weaker to a stronger binding site. The interatomic potential constructed by Becquart et al. [2] is validated by determining the interaction of carbon atoms with dislocations. According to Becquart's

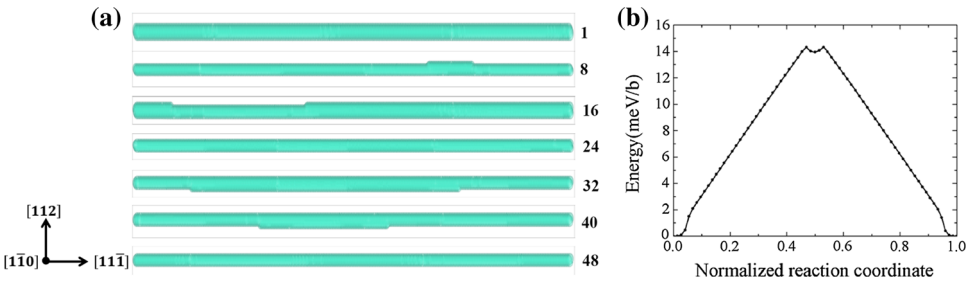

Figure 1 **a** Configuration change along the MEP during the kinking process without the manually constructed middle structure. The iron atoms in the dislocation core are shown as green spheres. **b** The energy of a $1/2[11\bar{1}]$ screw dislocation gliding along the MEP.

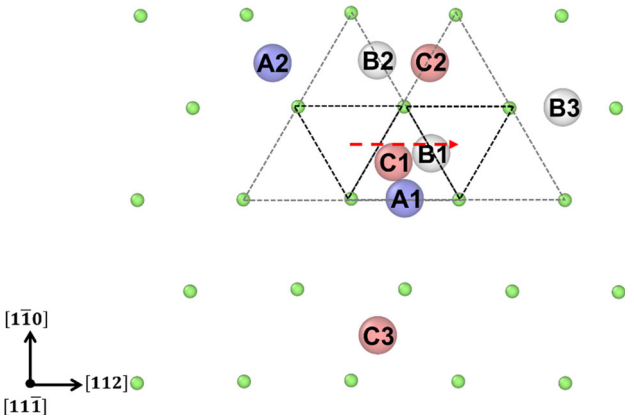

Figure 2 Atomic structure of a screw dislocation with the specific carbon interstitial positions discussed in this paper. Small green spheres represent Fe atoms, whereas larger spheres indicate carbon atoms. Blue, white, and red spheres indicate the binding sites A, B, and C for carbon atoms, respectively. The dislocation cores and second neighbor shells are visualized by black and gray-dashed lines, respectively. The red arrow indicates the gliding direction of the screw dislocation.

work, the binding energies of the eight sites are 0.41 eV for A1, − 0.14 eV for A2, 0.38 eV for B1, 0.39 eV for B2, 0.00 eV for B3, 0.22 eV for C1, − 0.14 eV for C2, and − 0.13 eV for C3 [2]. All structures are visualized and rendered using Open Visualization Tool (OVITO) [24]. The dislocation core is identified by dislocation extraction algorithm (DXA), a computational method developed by the author of OVITO [25].

Results

In our study, Fe screw dislocation with no carbon atom produced the double-kink formation mechanism during gliding. Regardless of the carbon atom, state 10 in Fig. 2 reveals the kink-pair mechanism of the screw dislocation without carbon, in which the two leading kinks, LA and LB, nucleated (here, the kink propagating along the positive $[11\bar{1}]$ direction is labeled as A, whereas the negative one is B). These were accompanied by the generation of two trailing kinks, TA and TB. All kinks propagated continually, as state 36 displays, and the width of the kink was $\sqrt{6}/3$ lattice constant. The minimum energy curve is displayed in Fig. 4a, which shows a shallow and wide intermediate valley and a barrier of 0.845 eV.

Carbon effect on kink-pair nucleation process

To study the effect of carbon on the kinking nucleation process, a carbon atom was placed at the site at one fourth the length of the dislocation line. Configurations along the located MEP with a carbon atom binding at eight positions are shown in Fig. 2. The dislocation moved from state 1 to 48 by kinking at the carbon atom from the initial to the final state. Regarding carbon positions A2, B3, and C3, which were outside the second neighbor shell of the dislocation core, the kink-pair nucleation mechanism was not influenced. Thus, the formation of LA and LB was maintained and accompanied by the generation of TA and TB. Considering carbon positions B1, B2, C1, and C2, which were inside the second neighbor shell of the dislocation core, the generation of LB was inhibited, whereas LA and TA formed initially. After the LA and TA propagated to a certain distance, LB and TB were generated. The unique behavior of position A1, where both the energies and relative distances between the carbon atom and screw dislocation remained the same at the initial and final states, revealed a process in which the LB and TB generated before LA and TA, which was quite different from all other cases. We noticed that, although

LA and LB did not generate simultaneously, the double-kink mechanism was not disturbed by the carbon interaction in all positions.

Regarding energy, Fig. 4a–c displays a change in energy of $1/2[11\bar{1}]$ screw dislocation along the MEP with the carbon atom influencing the kink-pair nucleation process. We noticed that the binding site of the carbon was stronger when the energy of the system was lower. Figure 4a shows that the postponed generation of LA and TA in position A1 resulted in an obvious increase in the kink generation barrier, whereas in position A2, no energy difference occurred because the carbon influence on the kink-pair nucleation mechanism could be neglected when the carbon was outside the second neighbor shell and the energy of the initial and final states was the same. Regarding positions B1, B2, and B3 in Fig. 4b, where the initial state yielded stronger binding for carbon, the kink-pair nucleation energies all increased. This phenomenon clarifies the fact that carbon increases the activation energy of kink-pair nucleation at a carbon atom when the carbon atom transits to a weaker binding site. Figure 4c displays the energy results of positions C1, C2, and C3, where the initial state was a weaker binding site for carbon. Regardless of the fact that the generation of LB and TB was prohibited at the preliminary stage at positions C1 and C2, the kink-pair nucleation barriers all decreased significantly. Carbon decreased the activation energy of kink-pair nucleation at a carbon atom when the carbon atom transits to a stronger binding site, and this in turn caused the mobility of screw dislocations to increase.

Carbon effect on kink-pair propagation process

Considering the carbon effect on the kink-pair propagation process, a carbon atom was placed at the midpoint of the length of the dislocation line. Configurations along the located MEP with a carbon atom binding at eight positions are shown in Fig. 4a–c. The kink-pair formation and propagation processes are displayed by atomic configurations from states 1 to 48. The double-kink nucleation remained valid in positions A1, A2, B2, B3, C1, and C3, as shown in state 14. However, in positions B1 and C2, only LB and TB generated and propagated as shown in state 14. Both positions B1 and C2 were on the side toward which the dislocation glides. At this location, carbon appeared to be a strong obstacle in the generation of LA and TA. Surprisingly, at state 30, LA and TA generated in position C2 and propagated toward LB and TB until the gliding of the screw dislocation finished. In position B1, TA and LA failed to nucleate during the entire process. All LA and TA kinks were inhibited by the carbon when migrating alongside it in positions A1, A2, B2, B3, C1, and C3. This indicates that carbon may considerably inhibit the propagation of a single kink, thus modifying the kink-pair mechanism to that of single kink. In addition, the influenced distance was greater than the nucleation process.

Figure 4d–f displays the energy change of the $1/2[11\bar{1}]$ screw dislocation along the MEP, with carbon atom affecting the kink-pair propagation process. Figure 4d shows that the postponed propagation of LA and TA results in a slight decrease in the kink propagation barrier in states A1 and A2. Although the kink propagation produced a barrier and the barrier decreased, the decrease effect on the kink propagation barrier could not be regarded as a carbon-enhanced mobility of screw dislocation. This is because the terminated single-kink propagation may more negatively affect mobility, resulting in an uncertain competition between these two inverse effects. This will be discussed further in a future study. As for positions B1, B2, and B3 in Fig. 4e, where carbon binds strongly at the initial state, the kink-pair propagation energies decreased at positions B2 and B3, just as they did at positions A1 and A2. Notice that in B1, the kink nucleation energy clearly decreased because the LA and TA did not generate during the gliding process. In real situations, B1 could act as a probable single-kink nucleation point. Since the kink nucleation energy clearly decreased when the carbon atom is at position B1, the single kink is energetically favorable to nucleate beside the carbon atom at B1 position. While the kink is supposed to generate at one fourth the length of the dislocation line, with the carbon atom located at B1, the single kink generated beside the carbon atom, which is at the midpoint of the length of the dislocation line instead, and double-kink mechanism did not occur during the whole process. The low kink nucleation energy and the changed kink nucleation point reveal that when carbon atom is at B1, the single-kink mechanism is preferred and the single

kink will generate beside the carbon atom. Figure 4f displays the energy results of positions C1, C2, and C3, where the carbon atom was at a weaker binding site in the initial state. Regarding the fact that the LA and TA were prohibited from generating at the preliminary stage at position C2, the kink-pair nucleation barriers decreased considerably as compared to the pure Fe condition. However, the kink nucleation energy remained unchanged for positions C1 and C3, and the kink propagation energy decreased when LA and TA were hindered. The carbon atom hindered the propagation of the single kink when the kink encountered the carbon during propagation, thus decreasing the mobility of screw dislocations.

Discussion

Based on the aforementioned results, the transition of the carbon binding positions at the dislocation core (which were caused by kinking) alters the activation energy of kink-pair nucleation. The possible binding positions for the carbon at different temperatures and the speed-controlling factors of the kink-pair mechanism under different conditions are first discussed for reference purposes. Because the diffusion ability of the carbon in an Fe matrix strongly depends on the temperature [2], at a low temperature like under 170 K, the mobility of carbon is decreased. Carbon will bind to the energy minimum site at the dislocation core and will not jump off. At a high temperature like 300 K, Veiga calculated the fractional occupancy of carbon atom per interstitial site surrounding the screw dislocation line, and the value is 0.1 in the core region ($R < 1$ nm), decreasing with increasing distance from the dislocation core [1]. Without considering those interstitial sites with a negative binding energy as C2 and C3 since the possibility of occupation is neglected, for dilute carbon solute, the possibility for the carbon atom to occupy the interstitial site with a binding energy as 0.22 eV (C1) is calculated according to the Maxwell–Boltzmann distribution modified by Louat [15, 29]:

$$\bar{n}_i = \frac{\frac{\bar{n}_0}{1-\bar{n}_0}\exp\left(\frac{E_b^i}{kT}\right)}{1+\frac{\bar{n}_0}{1-\bar{n}_0}\exp\left(\frac{E_b^i}{kT}\right)}$$

where $\bar{n}_i = n_i/N_i$, which represents the fractional occupancy of the interstitial sites with binding energy as E_b^i, and $\bar{n}_0 = n_0/N_0$ represents the fractional occupancy of the interstitial sites with binding energy as E_b^0. E_b^0 is the binding energy for a carbon atom very far away from the dislocation, which we take as 0 with the negligible interaction. Taking the temperature as 300 K, the possibility is quite large as 90%.

According to the previous examinations of the solid solution softening and hardening by mobile solute atoms [14], when the solute concentration is very low, the double-kink nucleation represents the rate-determination step, and softening occurs if the solute atoms segregate to kinks and reduce the kink formation energy. With increasing solute concentration, the rate of dislocation motion will finally be determined by the kink motion, and hardening will be observed when the kink motion is retarded by increasing solute drag. Besides, a common feature for BCC metals is the existence of a critical temperature: the knee temperature (T_k), under which the flow strength strongly depends on the temperature [21]. In bcc Fe, $T_k \approx 0.2T_M$, where T_M represents the melting point (1811 K). When the temperature is below $T_k = 362$ K, the nucleation of a kink pair requires much longer time than the propagation of the kink pair [5], and thus, the effect of the kink propagation could be neglected at these temperatures. Since the softening effect induced by carbon is between 150 and 300 K [6], which is below 362 K, basically we discuss the carbon-reducing kink generation barrier phenomenon to analyze the softening effect.

The atomistic process for carbon-induced softening and hardening is thus identified. When dilute carbon solute exits in an Fe matrix, the kink nucleation process represents the rate-determination step. At a low temperature, the carbon atoms will strongly bind to the energy minimum position around the dislocation core, which results in a considerable increase in the size of the kink nucleation barrier, as shown in Fig. 3e. At a high temperature, the mobility of the carbon solute increases, the binding with a weaker interstitial site as C1 and the screw dislocation gliding through it became possible, as the process shown in Fig. 3f, which decreases the activation energy of kink-pair nucleation. After this, softening occurs. This mechanism indicates that only a few carbon atoms on a typical dislocation segment are required to enhance the kink-pair nucleation and in turn the dislocation mobility. The binding sites for the carbon, which could decrease the energy of the system after the dislocation gliding through and the binding

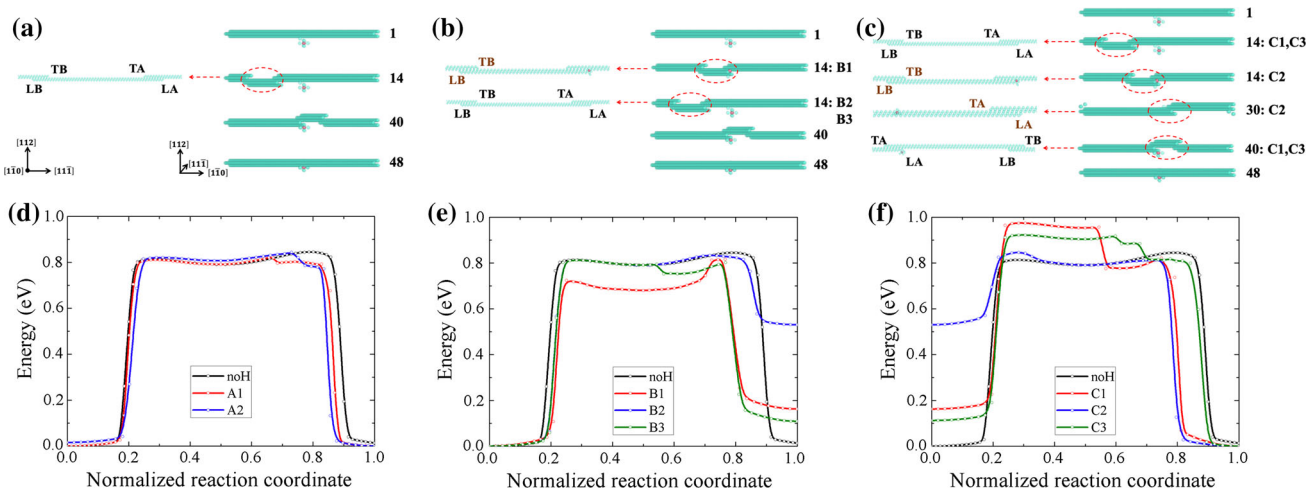

Figure 3 Configuration change along the MEP during the kinking process with a carbon atom binding at the kink generation site of position A1 and A2 (**a**), B1, B2 and B3 (**b**), C1, C2 and C3 (**c**), placing at the site at one fourth the dislocation length of the dislocation line. The iron and carbon atoms in the dislocation core are shown as green and red spheres, respectively. The left sets show enlarged images of the dislocation line surrounding the carbon atom in certain states. From 1 to 48, the screw dislocation migrates along the [112] direction with one-unit cell. State 10 with different behaviors related to the positions of the carbon atom are displayed for comparison. **d** Effect of carbon on the energy change of a $1/2[11\bar{1}]$ screw dislocation along the MEP: A carbon atom binding at position A1 and A2 is placed at the kink generation site at one fourth the length of the dislocation line. **e** A carbon atom binding at positions B1, B2, and B3 is placed at the kink generation site, reflecting the effect of the transition from a lower to a higher energy site. **f** A carbon atom binding at positions C1, C2, and C3 is placed at the kink generation site, reflecting the effect of the transition from a higher to a lower energy site.

energy is positive as C1, are those possible to contain a carbon atom and successfully decrease the kink nucleation barrier, which introduce the softening effects [9]. Meanwhile, the softening mechanism is further verified that the energy barriers for carbon atom to move between low- and high-energy binding sites around the core are larger compared to the kink formation energies. According to Veiga's work [28, Fig. 5] displays the map of the energy barriers for carbon migration in the vicinity of a straight screw dislocation. All the barriers are larger than 0.76 eV, including the moving between low- and high-energy binding sites. When the carbon atom binds at C1, the kink formation barrier will reduce to 0.63 eV as displayed in Fig. 3f from our work. Thus, the energy barriers for C moving between low- and high-energy binding sites around the core are larger compared to the kink formation energies when the carbon atom locates at C1 position, where the softening effect appears.

However, increasing the carbon solute enhances the solute drag effect on moving kinks, which in turn causes the kink propagation energy to become the rate-controlling factor. At a low temperature, the migration rate of carbon around screw dislocations is sufficiently lowered and carbon solutes may act as dragging points that impede the sideward motion of kinks. At a high temperature, the mobility of the carbon atom increases. Nevertheless, a possible jump from a weaker to a stronger binding site does not contribute to lower the kink formation energy, as shown in Fig. 4f. Although Fig. 4e reveals that the pinning of LA and TA could decrease the propagation barrier of the kink, with a high concentration of carbon solutes, this type of effect has to compete against the terminated single-kink propagation, which is a strong pinning effect produced by carbon atoms. The mobility of screw dislocations thus will decrease, and hardening occurs.

The interstitial impurities will influence the kink formation and motion process of the dislocation, further inducing the softening or hardening effects. This phenomenon also exists in other bcc metal-interstitial impurities systems, like tungsten–hydrogen and iron–hydrogen [14, 23, 33], which is linked to the hydrogen-enhanced local plasticity (HELP) or hydrogen embrittlement (HE). Similar discussion could be employed to explain the hardening and softening effects in these systems. At a high temperature and low hydrogen concentration, the plasticity

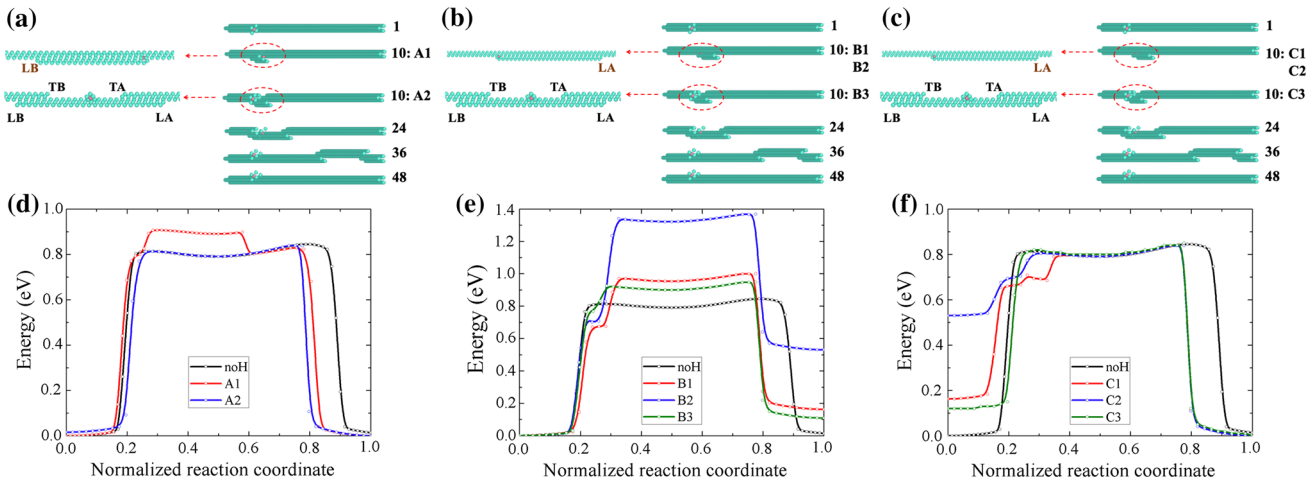

Figure 4 Configuration changes along the MEP in the kinking process with a carbon atom binding at the kink propagation site of position A1 and A2 (**a**), B1, B2, and B3 (**b**), C1, C2, and C3 (**c**), placing at the midpoint of the dislocation line. The iron atoms in the dislocation core are shown as green spheres, and the carbon atom is shown as the red sphere. The left sets show enlarged images of the dislocation line surrounding the carbon atom in certain states. From 1 to 48, the screw dislocation migrated along the [112] direction with one-unit cell. States 14 and 30 showing different behaviors related to the positions of the carbon atom are displayed for comparison. **d** Effect of carbon on the energy change of a $1/2[11\bar{1}]$ screw dislocation along the MEP: A carbon atom binding at positions A1 and A2 is placed at the kink propagation site, which is the midpoint of the dislocation line. **e** A carbon atom binding at positions B1, B2, and B3 is placed at the kink propagation site, reflecting the effect of the transition from a lower to a higher energy site. **f** A carbon atom binding at positions C1, C2, and C3 is placed at the kink propagation site, reflecting the effect of the transition from a higher to a lower energy site.

would be enhanced because the hydrogen reduced the kink formation energy in Fe or W. When the hydrogen concentration became higher, hydrogen embrittlement took place because the kink motion is hindered by the hydrogen solutes.

Conclusion

Atomistic simulations were conducted on the carbon-affected kinking process of a screw dislocation in iron. Specifically, the effects of carbon on the energetics of a kink-pair mechanism were simulated using the NEB method. We found that when a kink pair nucleated at a carbon atom, the activation energy decreased as the carbon atom transited to a stronger binding site, whereas the energy increased as the carbon atom transited to a weaker binding site. When the kink pair encountered a carbon atom during expansion, the sideward motion of the kink pair was impeded and the propagation barrier decreased, regardless of the relative energy difference between the initial and final states. We examined the softening and hardening effects while considering different temperatures and carbon solute concentrations. We found that with a dilute carbon solute and at a high temperature, a softening effect occurred when carbon atom located at some certain positions, whereas in other situations, the hardening effect was dominant.

Acknowledgements

This work was supported by National Magnetic Confinement Fusion Science Program of China under Grant 2013GB109004 and 2014GB117000 and by National Natural Science Foundation of China under Grant 51471092. The authors would like to acknowledge Danny Perez (LANL, New Mexico, USA) and Thomas D. Swinburne (LANL, New Mexico, USA) for technical assistance and helpful discussions. We appreciate Charlotte S. Becquart (ENSCL, Lille, France) for providing us the Fe–C EAM potential.

Compliance with ethical standards

Conflict of interest The authors declare no conflict of interest.

References

[1] Aguiar Veiga RGd (2011) Computational insights into the strain aging phenomenon in bcc iron at the atomic scale. Ph.D. thesis, Lyon, INSA

[2] Becquart C, Raulot JM, Bencteux G, Domain C, Perez M, Garruchet S, Nguyen H (2007) Atomistic modeling of an Fe system with a small concentration of C. Comput Mater Sci 40(1):119–129

[3] Becquart CS, Domain C (2011) Modeling microstructure and irradiation effects. Metall Mater Trans A 42(4):852–870

[4] Brown LM (2008) Strengthening mechanisms in crystal plasticity, by ali-argon. Contemp Phys 54(6):306–307

[5] Butler BG, Paramore JD, Ligda JP, Chai R, Fang ZZ, Middlemas SC, Hemker KJ (2018) Mechanisms of deformation and ductility in tungsten a review. Int J Refract Metals Hard Mater 75:248–261

[6] Caillard D (2011) An in situ study of hardening and softening of iron by carbon interstitials. Acta Mater 59(12):4974–4989

[7] Cereceda D, Diehl M, Roters F, Raabe D, Perlado JM, Marian J (2016) Unraveling the temperature dependence of the yield strength in single-crystal tungsten using atomistically-informed crystal plasticity calculations. Int J Plast 78:242–265

[8] Chaussidon J, Fivel M, Rodney D (2006) The glide of screw dislocations in bcc Fe: atomistic static and dynamic simulations. Acta Mater 54(13):3407–3416

[9] Clouet E, Garruchet S, Nguyen H, Perez M, Becquart CS (2008) Dislocation interaction with c in α-Fe: a comparison between atomic simulations and elasticity theory. Acta Mater 56(14):3450–3460

[10] Gilbert MR, Queyreau S, Marian J (2011) Stress and temperature dependence of screw dislocation mobility in a-Feby molecular dynamics. Phys Rev B 84(17):4193–4198

[11] Gordon PA, Neeraj T, Li Y, Li J (2010) Screw dislocation mobility in bcc metals: the role of the compact core on double-kink nucleation. Modell Simul Mater Sci Eng 18(18):085008

[12] Henkelman G, Johnsson H (2000) Improved tangent estimate in the nudged elastic band method for finding minimum energy paths and saddle points. J Chem Phys 113(22):9978–9985

[13] Hirth JP, Lothe J (1982) Theory of dislocations, 2nd edn. Wiley

[14] Kirchheim R (2012) Solid solution softening and hardening by mobile solute atoms with special focus on hydrogen. Scripta Mater 67(9):767–770

[15] Louat N (1956) The effect of temperature on cottrell atmospheres. Proc Phys Soc Sect B 69(4):459–467

[16] Monnet G (2005) Simulation of screw dislocation motion in iron by molecular dynamics simulations. Phys Rev Lett 95(21):215506

[17] Narayanan S, Mcdowell DL, Zhu T (2014) Crystal plasticity model for bcc iron atomistically informed by kinetics of correlated kinkpair nucleation on screw dislocation. J Mech Phys Solids 65(1):54–68

[18] Pink E, Arsenault RJ (1980) Low-temperature softening in body-centered cubic alloys. Prog Mater Sci 24(79):1–50

[19] Plimpton S (1995) Fast parallel algorithms for short-range molecular dynamics. J Comput Phys 117(1):1–19

[20] Proville L, Rodney D, Marinica MC (2012) Quantum effect on thermally activated glide of dislocations. Nat Mater 11(10):845–849

[21] Seeger A (2001) Why anomalous slip in body-centred cubic metals? Mater Sci Eng A 319(15):254–260

[22] Seeger A, Schiller P (1966) Kinks in dislocation lines and their effects on the internal friction in crystals. In: Mason WP (ed) Physical acoustics: principles and methods. Academic Press, New York

[23] Song J, Curtin WA (2013) Atomic mechanism and prediction of hydrogen embrittlement in iron. Nat Mater 12(2):145–151

[24] Stukowski A (2009) Visualization and analysis of atomistic simulation data with ovito-the open visualization tool. Modell Simul Mater Sci Eng 18(1):015012

[25] Stukowski A, Bulatov VV, Arsenlis A (2012) Automated identification and indexing of dislocations in crystal interfaces. Modell Simul Mater Sci Eng 20(8):085007

[26] Swinburne TD, Dudarev SL (2018) Kink-limited Orowan strengthening explains the brittle to ductile transition of irradiated and unirradiated bcc metals. Phys Rev Mater 2:073608. https://doi.org/10.1103/PhysRevMaterials.2.073608

[27] Trinkle DR, Woodward C (2005) The chemistry of deformation: how solutes soften pure metals. Science 310(5754):1665–1667

[28] Veiga RGA, Perez M, Becquart CS, Clouet E, Domain C (2011) Comparison of atomistic and elasticity approaches for carbon diffusion near line defects in a-iron. Acta Mater 59(18):6963–6974

[29] Veiga RGA, Perez M, Becquart CS, Domain C (2013) Atomistic modeling of carbon cottrell atmospheres in bcc iron. J Phys Condens Matter 25(2):025401

[30] Vitek V (2008) Paidar V (2008) Non-planar dislocation cores: a ubiquitous phenomenon affecting mechanical properties of crystalline materials. Dislocations Solids 14(07):439–514

[31] Vitek V (2010) Thermally activated motion of screw dislocations in BCC metals. Phys Status Solidi 18(2):687–701

[32] Weinberger CR, Boyce BL, Battaile CC (2013) Slip planes in bcc transition metals. Int Mater Rev 58(5):296–314
[33] Wen M, Fukuyama S, Yokogawa K (2003) Atomistic simulations of effect of hydrogen on kink-pair energetics of screw dislocations in bcc iron. Acta Mater 51(6):1767–1773

Publisher's Note Springer Nature remains neutral with regard to jurisdictional claims in published maps and institutional affiliations.